Spectral and Atmospheric Characterization of a Site at Atacama Desert for Earth Observation Sensor Calibration

Cibele T. Pinto, Flávio J. Ponzoni, C. Barrientos, C. Mattar, A. Santamaría-Artigas, and Ruy M. Castro

***Abstract*—The application of Earth observation sensor data in quantitative approaches calls on the conversion of original digital numbers to radiometric quantities such as radiance or reflectance. This conversion depends on the sensor absolute calibration. One of the postlaunch methods adopted to calibrate orbital sensors is the reflectance-based approach. According to this method, a reference surface with specifics characteristics is required. The main objective of this work is to evaluate the suitability of a specific surface located at Atacama Desert in Chile to be used as a reference surface for calibration of Earth observation sensor purposes. A field campaign was carried out from August 19 to 22, 2014, when radiometric measurements were performed to spectrally characterize the reference surface and to evaluate the atmospheric characteristics of the study area. The average reference surface reflectance factor in the spectral region from 350 to 2500 nm ranged from 0.1 to 0.3, and its spatial uniformity was within 2%–4%. The amount of atmospheric aerosols was low, with an aerosol optical depth at 550 nm between 0.08 and 0.11 during the fieldwork period. The climate is hyperarid, and the water column abundance was lower than 0.43 g/cm^2. The results demonstrated that a reference surface at Atacama Desert could be effectively used for calibration of either airborne or orbital electrooptical sensors, providing an excellent surface in South America.**

***Index Terms*—Atacama Desert, characterization, radiometric calibration, reflectance, sensor.**

I. Introduction

THE extraction of quantitative information from data collected by an Earth observation sensor is only possible through a well-performed absolute calibration procedure. One possible alternative for postlaunch absolute calibration is the reflectance-based method that has been successfully applied to several orbital sensors such as the Enhanced Thematic Mapper Plus (ETM+)/Landsat 7, the Advanced Spaceborne Thermal Emission and Reflection Radiometer (ASTER)/TERRA, the High Resolution CCD Camera (CCD)/CBERS-2, and the Operational Land Imager (OLI)/Landsat 8 [1]–[4].

This method requires a reference surface on the Earth that presents some relevant characteristics, which can be divided into two groups [1], [5]: 1) regional atmospheric and geographical characteristics must include low cloud cover rates and high altitude and must be flat, and 2) physical characteristics, such as high reflectance values and spatial and spectral uniformities. Furthermore, it is also desirable that the reference surface be easily accessible.

According to [6] and [7], desert surfaces (arid regions) are good candidates to be evaluated for orbital sensor calibration, especially for those that run on optical spectral ranges (visible, near-infrared, and shortwave-infrared). Therefore, the current study aims to evaluate the suitability of a specific surface located at Atacama Desert in Chile to be used for calibration of Earth observation sensor purposes. The evaluation was performed using ground radiometric measurements of the surface along with atmospheric measurements.

II. Atacama Desert

The Atacama Desert is located in the north region of Chile (Fig. 1), and it has not yet been explored for calibration purposes. The region presents an average elevation of 2400 m. Stretching 600 miles (1000 km), the Atacama is known as the driest place on Earth [8]. As observed by [9], the Atacama region presents low precipitation levels. In the station situated at Peine city, the annual precipitation was 23.1 mm between 1977 and 1991 [9].

The geographical coordinates of the reference surface are $23^\circ 08' 0.3'' $ S latitude and $68^\circ 03' 59''$ W longitude. The surface is $\sim$28 km south of San Pedro de Atacama city and easily accessible by road.

The size of the reference surface is chosen based on the spatial resolution of the sensor, i.e., the size of the chosen site must be compatible with the pixel size of the sensor that you desire calibrate. For ETM+/Landsat-7 and TM/Landsat 4 and 5, the sites were a rectangular area that is 480 m by 120 m [1]. The size of one site used to calibrate the OLI/Landsat-8 was 100 m by 250 m [4]. Here, a 300 m $\times$ 300 m surface was selected, which is the appropriate size to calibrate sensors with 30-m ground spatial resolution (or better resolution).

Manuscript received April 28, 2015; revised July 14, 2015; accepted July 21, 2015. Date of publication August 17, 2015; date of current version October 27, 2015.

C. T. Pinto and F. J. Ponzoni are with the Division of Remote Sensing, National Institute for Space Research (INPE), 12227-010 São José dos Campos, Brazil (e-mail: cibele@dsr.inpe.br; flavio@dsr.inpe.br).

C. Barrientos is with the Aerial Photogrammetric Service, Chile Air Force, Santiago, Chile (e-mail: carolina.barrientos@saf.cl).

C. Mattar and A. Santamaría-Artigas are with the Laboratory for Analysis of the Biosphere, Department of Environmental Sciences and Renewable Natural Resources, University of Chile, 1058 Santiago, Chile (e-mail: cmattar@uchile.cl; andres.santamaria.artigas@gmail.com).

R. M. Castro is with the Division of Geointelligence (EGI), Institute for Advanced Studies (IEAv/CTA), 12231-970 São José dos Campos, Brazil, and also with the Division of Mathematics and Physics, Universidade de Taubaté (UNITAU), 12201-970 Taubaté, Brazil (e-mail: rmcastro@ieav.cta.br; rmcastro@unitau.br).

Color versions of one or more of the figures in this paper are available online at http://ieeexplore.ieee.org.

Digital Object Identifier 10.1109/LGRS.2015.2460454

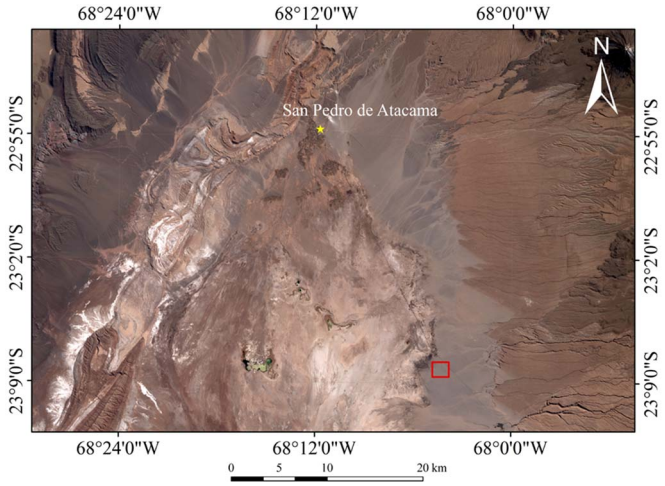

Fig. 1. Study area location. The box indicates the location of the field campaign surface.

III. Methodology

From August 19 to 22, 2014, a joint field campaign was conducted at Atacama Desert, and it involved three different institutions: Universidad de Chile, Servicio Aerofotogramétrico (SAF) from Chile, and National Institute for Space Research (INPE) from Brazil. INPE team collected the data used in this work. The data were collected on August; therefore, the data sample characterizes the specific chosen site of Atacama Desert and at this time of the year (winter in the Southern Hemisphere).

A. Atmospheric Characterization

The atmospheric characterization was performed using a manual Sun photometer CIMEL CE317 [10] running in five spectral bands: band 1 (1010–1030 nm), band 2 (860–880 nm), band 3 (660–680 nm), band 4 (430–450 nm), and band 5 (926–946 nm).

CIMEL CE317 converts the solar radiation generating an output signal V_λ, which can be modeled according to Beer's Law [11], [12]

$$V_\lambda = \frac{V_{0,\lambda} \times e^{-\tau_\lambda \times m}}{D^2} \tag{1}$$

where V_λ is the Sun photometer output, proportional to the solar irradiance for the wavelength λ; $V_{0,\lambda}$ is the calibration constant for the wavelength λ; D is the Sun–Earth distance factor in astronomical units; m is the relative optical airmass; and τ_λ is the total optical depth for the wavelength λ.

To estimate the influence of the atmosphere using (1), it is necessary to determine the $V_{0,\lambda}$ and τ_λ values. Therefore, the Langley method was used, which consists in the linearization of Beer's law

$$\ln(V_\lambda \times D^2) = \ln(V_{0,\lambda}) - m \times \tau_\lambda. \tag{2}$$

According to this law, if a series of measurement is performed for different optical air masses and during a time period where the total optical depth remains constant, then it is possible to estimate $V_{0,\lambda}$ and τ_λ. The Langley method results in a linear fitting, where the linear coefficient is the natural logarithm of $V_{0,\lambda}$ and the slope coefficient is τ_λ.

The total optical depth τ_λ is the attenuation result by molecules (Rayleigh scattering), aerosols, ozone, water vapor, and other mixed gases [12]. The Rayleigh component depends only on the wavelength and barometric pressure at the surface level. The effect of ozone and other mixed gases can be ignored since the Sun photometer runs on a different spectral range [12]. Absorption by water vapor is restricted to narrow spectral bands, i.e., in this case, band 5.

Therefore, the aerosol optical depth $\tau_{\mathrm{Aerossol},\lambda}$ can be obtained by the subtraction of the Rayleigh $\tau_{\mathrm{Rayleigh},\lambda}$ from the total optical depth

$$\tau_{\mathrm{Aerossols},\lambda} = \tau_\lambda - \tau_{\mathrm{Rayleigh},\lambda}. \tag{3}$$

According to the Angström's turbidity formula [12], the spectral variation of the aerosol optical depth can be written as

$$\tau_{\mathrm{Aerossols},\lambda} = \beta \times \lambda^{-\alpha} \tag{4}$$

where α is the exponent Ångström related to the average size distribution of the aerosols and β is an Ångström turbidity parameter, which is proportional to both the amount of aerosols and the horizontal visibility VIS (km), as shown by the following [13]:

$$\beta = 0,613 \times e^{-\frac{VIS}{15}}. \tag{5}$$

The Sun photometer spectral range centered at approximately 936 nm (band 5) was used to estimate the water vapor atmospheric content. However, (1) is not valid throughout the spectral region of absorption by water vapor. In this case, the Sun photometer output $V_{936\ \mathrm{nm}}$ is estimated using [14]

$$V_{936\ \mathrm{nm}} = \frac{V_{0,936\ \mathrm{nm}} \times e^{-\tau_{936\ \mathrm{nm}} \times m}}{D^2} \times T_W \tag{6}$$

where $V_{936\ \mathrm{nm}}$ is the Sun photometer output at 936 nm, $V_{0,936\ \mathrm{nm}}$ is the calibration constant at 936 nm, $\tau_{936\ \mathrm{nm}}$ is the total optical depth at 936 nm, and T_W is the gaseous transmittance, which can be estimate using the following expression [13]:

$$T_W = e^{-a \times W^b \times m^c} \tag{7}$$

where W is the water vapor content (in grams per square centimeter) and a, b, and c are constants, which depend on the equipment used, i.e., b and c are approximately equal to 0.5.

To determine the $V_{936\ \mathrm{nm}}$ and W values, the Langley modified method has been applied [12], [14]. Thus, (6) can be rewritten as

$$\ln(V_{936\ \mathrm{nm}} \times D^2) + m \times \tau_{936\ \mathrm{nm}} = \ln(V_{0,936\ \mathrm{nm}}) - a \times W^b \times m^c. \tag{8}$$

A plot of the left side of (8) against m^c yields a straight line, with the ordinate intercept equal to $\ln(V_{0,936\ \mathrm{nm}})$ and the slope equal to $a \times W^b$.

The CIMEL CE317 measurements were performed during every day of the field campaign, according to the schedule presented in Table I. The weather on these days was clear with no clouds. Measurements were made at intervals of approximately 5 min.

As can be seen in Table I, the measurements with the Sun photometer on the first day (August 19, 2014) were performed from sunrise until sunset. Thus, the data collected from this day were utilized to calibrate the instrument (CIMEL/CE-317),

TABLE I
SUN PHOTOMETER MEASUREMENT SCHEDULE, JULIAN DAY (J), AND PRESSURE (P)

Day	08/19/2014	08/20/2014	08/21/2014	08/22/2014
Local Time	7h15-18h00	9h30-11h30	9h15 -12h15	9h30 - 11h30
J	231	232	233	234
P (hPa)	763.8 ± 1.4	764.1 ± 0.8	764.0 ± 0.9	763.8 ± 0.9

i.e., they were used to determine the calibration constant $V_{0,\lambda}$ according to (1).

B. Reference Surface Spectral Characterization

A 3000 m × 300 m surface where 25 sample points have been uniformly positioned was selected. To obtain the surface reflectance, an Analytical Spectral Devices (ASD) spectroradiometer and a Spectralon reference panel from Labsphere were used [15], [16].

The radiometric measurements were performed only by hands, trying to maintain the sensitive radiometer device at 1.3 m high. The operator has avoided the projection of his shadow on the area to be effectively measured. The reference panel was kept on a tripod near each sample point on a horizontal position. These radiometric measurements from the 25 sample points were performed from 10:00 to 11:00 A.M. (local time) every day.

The reflectance factor RF_{surface} of the site was determined by ratioing the radiance from the surface L_{surface} by the radiance from the reference panel L_{panel}

$$RF_{\text{surface}} = \frac{L_{\text{surface}}}{L_{\text{panel}}} \times k \tag{9}$$

where k is the panel correction factor (estimated in the laboratory). For simplification purposes, the spectral and angular dependences of RF were omitted.

In order to determine the operational conditions of the instruments and their respective contributions to the total uncertainties, in-lab radiometric measurements both before and after the field campaign were also carried out at the Radiometry and Characterization of Electro-optical Sensors Laboratory (LaRaC), Institute for Advanced Studies (IEAv), located in São José dos Campos, São Paulo, Brazil. In the experiment conducted at LaRaC, the Spectralon reference panel and ASD FieldSpec Pro spectroradiometer used in the field were evaluated against similar equipment belonging to LaRaC.

C. Uncertainties

Confidence in a measurement value requires a quantitative report of its quality, which, in turn, demands the evaluation of the uncertainty associated with the value. Thus, it is important to note that the ground radiometric measurements of the surface along the atmospheric measurements are incomplete unless accompanied by a statement of their uncertainties.

Here, the classical method of propagation of uncertainties described in the Guide to the Expression of Uncertainty in Measurement, known as the GUM [17], was applied. It was developed by the Joint Committee for Guides in Metrology, a joint committee of all of the relevant standards organizations (ISO) and the Bureau International des Poids et Mesures (BIPM). The GUM provides guidance on how to determine, combine, and express uncertainties that are intended to be applicable to a wide range of measurements.

The propagation law of uncertainty was applied when the quantity was calculated indirectly. If $y = f(x_1, x_2, \ldots, x_n)$ and $x_1, x_2, \ldots, x_n$ are quantities with uncertainties $\sigma_{x1}, \sigma_{x2}, \ldots, \sigma_{xn}$, then the uncertainty of quantity f is

$$\sigma_f^2 = \sum_{i=1}^{n} \left(\frac{\partial f}{\partial x_i}\right)^2 \times \sigma_{x_i}^2 + 2 \times \sum_{i=1}^{n-1} \sum_{j=i+1}^{n} \frac{\partial f}{\partial x_i} \frac{\partial f}{\partial x_j} \times \sigma_{x_i x_j} \tag{10}$$

where $\partial f / \partial x_i$ are the partial derivatives, often referred to as sensitivity coefficients; σ_{x_i} is the standard uncertainty associated with the input estimate x_i; and σ_{xixj} is the estimated covariance associated with x_i and x_j. If the variables $x_1, x_2, \ldots, x_n$ are uncorrelated, the covariance is equal to zero.

As usually done in sensor calibration works [18], the uncertainty values were quoted as one-sigma percentages (confidence level of 68.3%).

IV. RESULTS AND DISCUSSION

Fig. 2(a) shows the mean reflectance factor of the reference surface at Atacama Desert versus wavelength. In addition, the coefficient of variation (CV) defined as the ratio between the standard deviation and the average is shown as a percent [Fig. 2(b)].

According to [5], reflectance values higher than 0.3 in the entire spectral range are preferred. As it can be seen in Fig. 2(a), the average reference surface reflectance factor is between 0.11 and 0.25 from 350 to 1000 nm and about 0.30 from 1000 to 2500 nm. Reference [19] has presented reflectance spectral curves from the Railroad Valley Playa and Niobrara, NE, USA. The Nebraska test site did not present a reflectance higher than that value in almost all of the spectral range from 300 to 2500 nm. Despite that, data from the Niobrara surface have been considered in calibration campaigns [20], [21].

Scott *et. al* [5] suggest that a certain surface is sufficiently spatially uniform if the CV is lower than 5%. Here, the average CV of the spectral measurements ranged from 2.12% to 3.99% for all four days of fieldwork, indicating that the reference surface at Atacama Desert presents a spatial uniformity better than 4%.

Fig. 3 shows the Langley method graphs obtained with the data collected on August 19, 2014, for bands 1, 2, 3, and 4 of the CE317/CIMEL. Table II shows the total optical depth and the aerosol optical depth for all four days of fieldwork and for each Sun photometer spectral band.

Tiny solid and liquid particles suspended in the atmosphere are called aerosols. An aerosol optical depth lower than 0.1 indicates clear sky, whereas a value of 1 corresponds to very hazy conditions. The highest value found was on August 19, 2014, for band 4 (440 nm): 0.133 ± 0.003. Therefore, the Atacama Desert presents low aerosol loading.

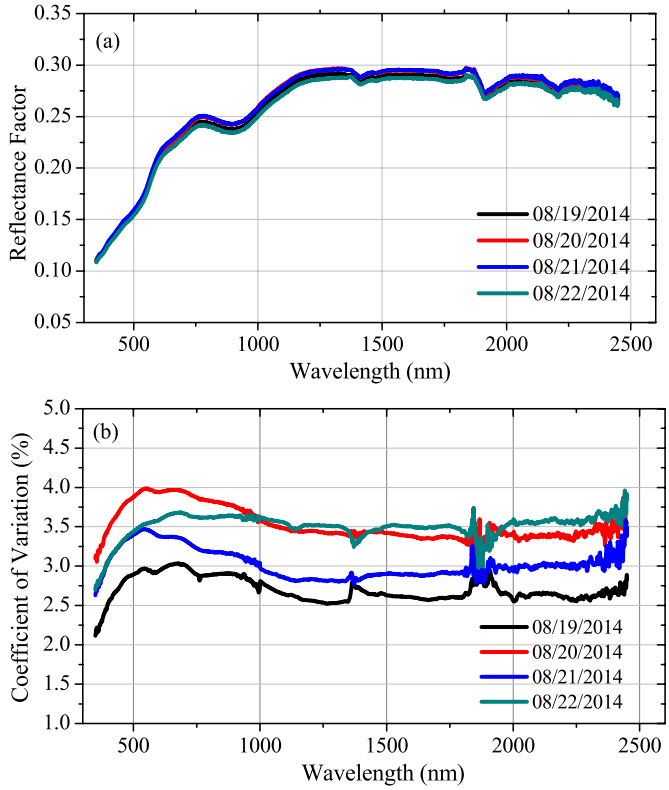

Fig. 2. (a) Spectral reflectance factor of the reference surface at Atacama Desert. (b) Relative CV.

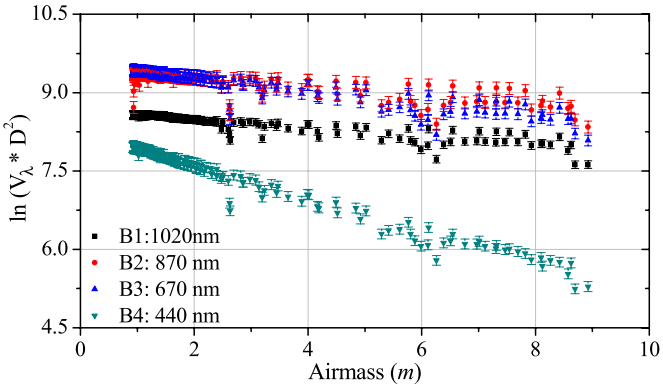

Fig. 3. Langley graph for bands 1, 2, 3, and 4 of the CIMEL CE317 Sun photometer.

The total optical depth accuracy (consequently the accuracy of aerosol optical depth) depends on the following: 1) the calibration of the Sun photometer and 2) the stability of the atmospheric conditions during the period of measurements.

According to [18], the uncertainty in measurements made with a Sun photometer should be no more than 5%. As mentioned previously, the data collected on August 19, 2014, were used to calibrate the instrument (CIMEL/CE-317); therefore, the uncertainties in that day were the largest but lower than 4.71% (band 870 nm) in the total optical depth. Regarding the total aerosol depth uncertainties, they ranged from 0.92% (band 440 nm on August 22, 2014) to 5.41% (band 870 nm on August 19, 2014).

TABLE II
TOTAL OPTICAL DEPTH τ_λ AND THE AEROSOL OPTICAL DEPTH $\tau_{\mathrm{Aerossol},\lambda}$

Band nm	τ_λ	$\tau_{Aerossol,\lambda}$
08/19/2014		
1020	0.0849 ± 0.0023	0.0789 ± 0.0023
870	0.085 ± 0.004	0.074 ± 0.004
670	0.132 ± 0.003	0.099 ± 0.003
440	0.3162 ± 0.0029	0.133 ± 0.003
08/20/2014		
1020	0.1050 ± 0.0012	0.0989 ± 0.0012
870	0.0675 ± 0.0009	0.0561 ± 0.0009
670	0.1237 ± 0.0010	0.0908 ± 0.0010
440	0.3018 ± 0.0012	0.1187 ± 0.0014
08/21/2014		
1020	0.0781 ± 0.0009	0.0721 ± 0.0009
870	0.0442 ± 0.0011	0.0328 ± 0.0011
670	0.0972 ± 0.0014	0.0643 ± 0.0014
440	0.2665 ± 0.0009	0.0835 ± 0.0012
08/22/2014		
1020	0.0877 ± 0.0011	0.0817 ± 0.0011
870	0.0501 ± 0.0006	0.0386 ± 0.0006
670	0.1034 ± 0.0007	0.0705 ± 0.0007
440	0.2808 ± 0.0005	0.0978 ± 0.0009

TABLE III
HORIZONTAL VISIBILITY VIS, THE AEROSOL OPTICAL DEPTH AT 550 nm $\tau_{\mathrm{Aerossol},550\ \mathrm{nm}}$, AND THE WATER CONTENT W

Day	*VIS* (km)	$\tau_{Aerossol,550nm}$	W (g/cm^2)
08/19/14	31.3 ± 0.8	0.114 ± 0.009	0.429 ± 0.020
08/20/14	33.0 ± 1.8	0.102 ± 0.014	0.4318 ± 0.0023
08/21/14	37.4 ± 2.4	0.076 ± 0.013	0.2986 ± 0.0010
08/22/14	37.2 ± 2.1	0.077 ± 0.012	0.4267 ± 0.0018

A fitting was applied using the Ångström formula (4), and from the Ångström parameters, we determined the horizontal visibility VIS and the aerosol optical depth at 550 nm $\tau_{\mathrm{Aerossol},550\ \mathrm{nm}}$. The results can be seen in Table III.

Columnar water vapor was derived from the solar extinction data using a modified Langley approach (see Fig. 4). The water content was lower than 0.43 g/cm^2 for the four days, and its uncertainties ranged from 0.33% to 4.66% (Table III). Fig. 2 shows no gaps in the reflectance and the standard deviation curve in the spectrum regions strongly affected by water vapor absorption (around 1400 and 1900 nm). This means that the amount of water is very low in this region.

Thome [1] reports the results from ground-based measurements of atmospheric conditions made at Railroad Valley Playa, Nevada, Roach Lake Playa, Nevada, and White Sands Missile Range, New Mexico. For comparison purposes, the column water vapor in these sites ranged from 0.758 to 1.595 g/cm^2, and

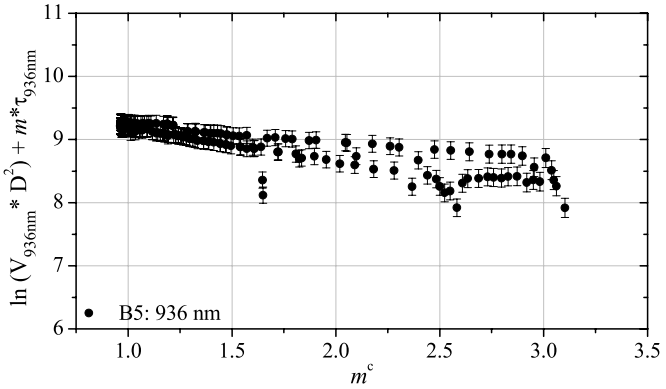

Fig. 4. Modified Langley graph with data collected on August 19, 2014.

the 550-nm aerosol optical depth was between 0.0207 and 0.1024.

V. Conclusion

Applying the reflectance-based approach for Earth observation sensor calibration is necessary to select a surface on the Earth with specific characteristics. This study focuses on evaluating a site at Atacama Desert in Chile for postlaunch calibration purposes.

According to ideal vicarious calibration site characteristics, the surface explored here, located at Atacama Desert, seems be a good reference surface because of the following: 1) it is sufficiently large; 2) it is located at a high altitude, with a very low amount of atmospheric aerosols (aerosol optical depths at 550 nm lower than 0.11); 3) it has high spatial uniformity (better than 4%); 4) it is hyperarid (the water column abundance was lower than 0.43 g/cm^2); 5) it has high probability of clear weather; 6) it has a flat site with almost no vegetation; and 7) the accessibility is easy. The only characteristic that could be considered a disadvantage is that the surface evaluated did not present high reflectance values. In the spectral region from 350 to 2500 nm, the reflectance is about 0.11 to 0.30. However, it is important to note that no surface is able to fulfill all requirements for a "perfect" site reference. Therefore, the surface can be utilized as a radiometric calibration test site for optical sensors in the solar reflected spectrum.

It is noteworthy that the spectral reflectance and atmospheric characterization evaluation of Atacama Desert were performed at ground level during four consecutive days in August 2014. The collected data describe the specific chosen site at Atacama Desert and at this time of the year (winter in the Southern Hemisphere). This work was the first study in order to characterize the Atacama Desert for sensor calibration purposes, and the results were encouraging. Therefore, in future studies, intend to collect sample data (ground and satellite level) in different months and in areas throughout Atacama Desert, in such a way that it can be wholly characterized.

Acknowledgment

The authors would like to thank Conselho Nacional de Desenvolvimento Científico e Tecnológico (CNPq) and the Coordenação de Aperfeiçoamento de Pessoal de Nível Superior (CAPES) for the scholarship given to C. T. Pinto and the research financial support and the project Fondecyt-Initial (CONICYT ref./11130359).

References

[1] K. J. Thome, "Absolute radiometric calibration of Landsat-7 ETM+ using the reflectance-based method," *Remote Sens. Environ.*, vol. 78, no. 1/2, pp. 27–38, Apr. 2001.

[2] K. J. Thome, K. Arai, S. Tsuchida, and S. F. Biggar, "Vicarious calibration of ASTER via the reflectance based approach," *IEEE Trans. Geosci. Remote Sci.*, vol. 46, no. 10, pp. 3285–3295, Oct. 2008.

[3] F. J. Ponzoni, J. Zullo, Jr., and R. A. C. Lamparelli, "In-flight absolute calibration of the CBERS-2 CCD sensor data," *Ann. Brazilian Acad. Sci.*, vol. 80, no. 2, pp. 373–380, Jun. 2008.

[4] J. Czapla-Myers *et al.*, "The ground-based absolute radiometric calibration of Landsat 8 OLI," *Remote Sens.*, vol. 7, no. 1, pp. 600–626, Jan. 2015.

[5] K. P Scott, K. J. Thome, and M. R Bronwlee, "Evaluation of the railroad valley playa for use in vicarious calibration," in *Proc. SPIE*, Aug. 1996, vol. 2818, pp. 158–166.

[6] H. Cosnefroy, M. Leroy, and X. Briottet, "Selection and characterization of Saharan and Arabian desert sites for the calibration of optical satellite sensors," *Remote Sens. Environ.*, vol. 58, no. 1, pp. 101–114, Oct. 1996.

[7] L. H Dennis, B. Bikash, and L. M. Daniel, "Optimized identification of worldwide radiometric pseudo-invariant calibration sites," *Can. J. Remote Sens.*, vol. 36, no. 5, pp. 527–539, Jun. 2010.

[8] P. J. Vesilind, "The driest place on Earth," *Nat. Geogr.*, vol. 204, no. 2, pp. 46–71, Aug. 2003.

[9] J. Houston and A. J. Hartley, "The central Andean west-slope rainshadow and its potential contribution to the origin of hyper-aridity in the Atacama Desert," *Int. J. Climatol.*, vol. 23, no. 12, pp. 1453–1464, Aug. 2003.

[10] R. A. C. Lamparelli, F. J. Ponzoni, J. Zullo, G. Q Pellegrino, and Y. Arnaud, "Characterization of the Salar de Uyuni for in-orbit satellite calibration," *IEEE Trans. Geosci. Remote Sci.*, vol. 41, no. 6, pp. 1461–1468, Jun. 2003.

[11] B. Schmid and C. Wehrli, "Comparison of Sun photometer calibration by use of the Langley technique and the standard lamps," *Appl. Opt.*, vol. 34, no. 21, pp. 4500–4512, Jul. 1995.

[12] E. M. Rollin, "An introduction to the use of Sun-photometry for the atmospheric correction of airborne sensor data," in *Proc. Annu. Meet. NERC EPFS NERC ARSF*, Nottingham, U.K., 2000, p. 22.

[13] F. J. Ponzoni, C. T. Pinto, R. A. C. Lamparelli, J. Zullo, Jr, and M. A. H. Antunes, *Calibração de Sensores Orbitais*, 2nd ed. São José dos Campos, Brazil: Oficina de Textos, 2015, p. 96.

[14] R. N. Halthore, T. F. Eck, B. N. Holben, and B. L. Markham, "Sun photometric measurements of atmospheric water vapor column abundance in the 940-nm band," *J Geophys. Res. Atmos.*, vol. 102, no. D4, pp. 4343–4352, Feb. 1997.

[15] Analytical Spectral Devices Technical Guide, 3rd ed., Analytical Spectral Devices, Boulder, CO, USA, 1999, p. 140.

[16] Setting the Standard in Light Measurement: Product Guide, Labsphere Inc., Sutton, New Hampshire, USA, 2009, p. 28.

[17] Evaluation of Measurement Data—Guide to the Expression of Uncertainty in Measurement, JCGM 100:2008, 1st. ed., Joint Committee for Guides in Metrology and Bureau International des Poids et Mesures, p. 134 , 2008.

[18] S. F. Biggar, P. N. Slater, and D. I. Gellman, "Uncertainties in the in-flight calibration of sensors with reference to measured ground sites in the 0.4-1.1 μm range," *Remote Sens. Environ.*, vol. 48, no. 2, pp. 245–252, May 1994.

[19] P. M. Teillet *et al.*, "Radiometric cross-calibration of the Landsat-7 ETM+ and Landsat-5 TM sensors based on tandem data sets," *Remote Sens. Environ.*, vol. 78, no. 1, pp. 39–54, Apr. 2001.

[20] J. E. Vogelmann *et al.*, "Effects of Landsat 5 thematic mapper and Landsat 7 enhanced thematic mapper plus radiometric and geometric calibrations and corrections on landscape characterization," *Remote Sens. Environ.*, vol. 78, no. 1/2, pp. 55–70, Oct. 2001.

[21] P. M. Teillet, G. Fedosejevs, and K. J. Thome, "Spectral band difference effects on radiometric cross-calibration between multiple satellite sensors in the Landsat solar-reflective spectral domain," in *Proc. SPIE*, Nov. 2004, vol. 5570, pp. 307–316.